

STUDIES OF THE NUCLEON-NUCLEUS AND THE NUCLEON-NUCLEON INTERACTIONS  
USING POLARIZED NEUTRON BEAMS

R.L. Walter, C.R. Howell and W. Tornow

Department of Physics, Duke University, Durham, North Carolina, 27706  
U.S.A.and  
Triangle Universities Nuclear Laboratory, Durham, North Carolina, 27706  
U.S.A.

**Abstract:** The results of four scattering measurements using beams of polarized neutrons are described. Results for the analyzing power  $A_y(\theta)$  for elastic scattering of neutrons from protons and deuterons are compared to calculations based on the Paris and the Bonn nucleon-nucleon interactions. Deficiencies particularly in the Bonn model are indicated. A nucleon-nucleus potential is derived from  $\sigma(\theta)$  and  $A_y(\theta)$  data for  $n + {}^{28}\text{Si}$  and  $p + {}^{28}\text{Si}$  and the Coulomb correction terms are derived according to two approaches. A Fourier-Bessel expansion is used to investigate the form factors of the terms of the  $n + {}^{208}\text{Pb}$  potential which are necessary to describe  $\sigma(\theta)$  and  $A_y(\theta)$  data from 6 to 10 MeV. The nature of the spin-orbit term is also presented.

(scattering of polarized neutrons, nucleon-nucleon force, neutron-nucleus interaction, Coulomb correction terms,  $n + {}^{208}\text{Pb}$  potential)

Introduction

Polarization studies involving neutron beams as probes have been performed at Triangle Universities Nuclear Laboratory (TUNL) for a wide variety of interactions. The use of polarized beams not only allows one to precisely study spin-sensitive parts of the nuclear force, but also gives an excellent probe for selecting specific angular momentum states in nuclear processes. The present paper will illustrate a few examples of the types of fundamental information obtained and the quality of the data presently attainable in experiments involving 5- to 20-MeV neutrons.

The TUNL investigations exploit unique aspects of the neutron-nucleus interaction related either to the isospin structure of neutrons or to their neutral charge state. The following observations are made to emphasize the importance of using neutrons as a probe of the nuclear force and to introduce some of the projects currently underway at TUNL: i) Measurements of the n-p scattering observables give the most direct measure of the  $T=0$  part of the nucleon-nucleon interaction. Since neutron targets are unavailable for studying the  $n(p,p)n$  process, neutron beams scattered from proton targets, that is,  $p(n,n)p$ , is the scattering process we use to investigate this term. ii) At the present time it is impossible to treat exactly the long-range Coulomb interaction between charged-particles in few-nucleon reactions. Because the accuracies of the approximations used in such calculations are uncertain, it is difficult to interpret discrepancies between theoretical predictions and measurements with proton and deuteron beams. iii) The isovector terms, i.e. asymmetry terms, in the nucleon-nucleus interaction, which are proportional to  $(N-Z)/A$ , must be consistent for

both neutron and proton projectiles. Hence, it is necessary to have neutron scattering data available for characterizing these terms. iv) Measurements of the spin-spin part of the nucleon-nucleus interaction can only be done to high accuracy with neutron beams. Such experiments are being conducted at TUNL by the group of Gould, Roberson and Haase. These studies, which involve polarized neutrons incident on large volume polarized targets, have given new information on the spin-spin interaction<sup>1</sup> for  ${}^{27}\text{Al}$  and  ${}^{93}\text{Nb}$ . Because of the brevity constraint on the present paper, these latter experiments will not be discussed here.

The polarization observables illustrated in the present paper are confined to the vector analyzing power  $A_y(\theta)$ . This quantity is defined as the difference between differential cross sections for scattering to the left side and right side divided by their sum when the incident neutron beam is 100% polarized with the spin orientation normal to the scattering plane. That is,  $A_y(\theta) = [\sigma_L(\theta) - \sigma_R(\theta)] / [\sigma_L(\theta) + \sigma_R(\theta)]$ . The denominator is equal to twice the usual differential cross section  $\sigma(\theta)$  obtained with unpolarized beams. Since  $A_y(\theta)$  is simply a ratio of cross sections, by alternately changing the spin orientation of the incoming neutron beam from up to down, the experiments can be performed in such a way that the efficiency of the detectors cancels. This allows one to measure values of  $A_y$  to an absolute accuracy of  $\pm 0.002$  with present methods. This is an order of magnitude better than people report for absolute measurements of  $\sigma(\theta)$  for neutron scattering.

At TUNL the polarized neutron beam is produced by the  ${}^2\text{H}(\bar{d},n){}^3\text{He}$  reaction at  $0^\circ$ , where the symbol  $\bar{d}$  is used here to indicate that the reaction is initiated with vector polarized deuterons. At TUNL the deuteron polarization is typically

67%, yielding neutron beams with about 60% polarization. The measurements are performed in the tandem Van de Graaff laboratory and "monoenergetic" neutron beams are available between 5 and 19 MeV with this source reaction. Time-of-flight spectroscopy is employed with up to 3 neutron detectors on each side (left and right) of the scattering target.

#### Few-Nucleon Investigations

In the area of few-nucleon studies, we have made new observations of  $A_y(\theta)$  for n-p and n-d elastic scattering. We have also measured  $A_y(\theta)$  for n+d breakup processes for configurations which correspond to n-p quasifree scattering and to nucleon-nucleon final-state interactions. Renewed motivation for this work comes from theoretical and computational developments which now permit rigorous calculations<sup>2</sup> using "realistic" potentials<sup>3</sup> based on meson exchange. Problems of exactly incorporating the long-range Coulomb interaction in p+d reactions still hamper the direct comparisons of p-d data to theoretical calculations; therefore the neutron data plays an important role in developing our understanding of few-nucleon systems.

In this section comparisons of data will be made to calculations based on several important approaches for describing the basic nucleon-nucleon (NN) interaction. One is a straightforward phase-shift analysis of available NN scattering data. This approach is frequently updated, the most current being the 1987 analysis of Arndt<sup>4</sup>, who includes NN data up to 1 GeV in his phase shift search. Another method is to represent the nuclear force with a semi-phenomenological potential. One important work along this line is that of the group at Paris, who published<sup>5</sup> in 1980 a model based on a one-boson-exchange potential that was supplemented with a phenomenological short-range interaction and  $2\pi$ -exchange contributions. A third approach is one based on field-theory. The Bonn group<sup>3</sup> adopted this more explicit method and recently reported a representation of the nuclear force which includes the usual one- and two-meson exchange terms, but also includes nucleon-meson-isobar vertices and relevant  $3\pi$ - and  $4\pi$ -exchange diagrams. This work also forms a solid basis for a consistent calculation of the three-nucleon forces. A noteworthy breakthrough with this model is that it predicts the correct value for the triton binding energy; this quantity is underestimated by about 1 MeV by all the other previous nucleon-nucleon (NN) potentials, such as the favored Paris potential<sup>5</sup>.

The TUNL measurements of  $A_y(\theta)$  for n-p scattering at 16.9 MeV are shown in Fig. 1. The data set contains four new points<sup>6</sup> between 135° and 165° and some previously reported points, several of which were recently revised<sup>6</sup> to account for two subtle multiple-scattering effects that produce instrumental asymmetries, but

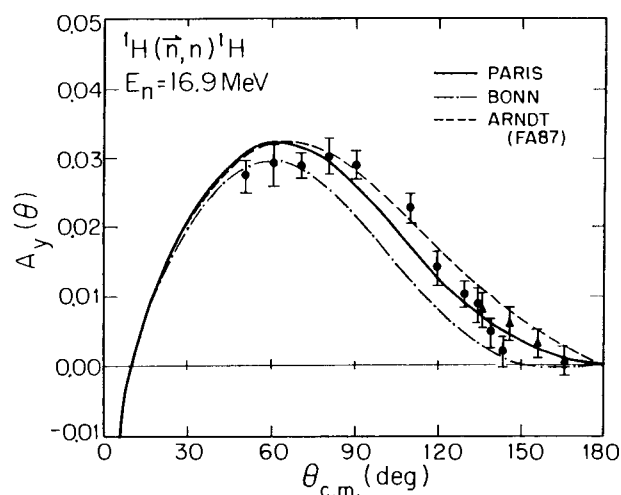


Fig. 1 Analyzing power for n-p scattering at 16.9 MeV.

which had been neglected earlier. Predictions from the three models mentioned above are shown in Fig. 1. Clearly, none of the calculations follow the systematics of the data perfectly. The prediction based on the Paris semi-phenomenological potential gives the most reasonable description of the data. The prediction based on the newest potential, the Bonn potential, is not compatible with the data. The problem most likely arises from the size of the triplet p-wave ( $^3P$ ) NN interaction generated with this model. We have just initiated a project to measure  $A_y(\theta)$  at lower energies to a slightly higher accuracy than that shown in Fig. 1 to obtain a good definition of  $A_y(\theta)$  as a function of  $E_n$ .

The interaction of polarized neutrons with deuterons not only gives additional information about the nucleon-nucleon force, but also is the main probe of the three-nucleon force (3NF). Since the 3NF acts mainly through a  $^3P$  interaction, it is important to measure observables that are particularly sensitive to  $^3P$  interactions. Neutron-deuteron scattering experiments below 20 MeV fall into this category because here s- and p-wave interactions dominate.

Calculations<sup>7</sup> of  $A_y(\theta)$  for n-d elastic scattering have been made at TUNL using the code of Y. Koike which is based on the Faddeev method. First, a separable approximation of the Paris NN potential, referred to as PEST, was chosen. The results for 12 MeV are shown as the solid curve in Fig. 2 alongside data obtained at TUNL. Except in the region near 125°, the calculation looks extremely good. At 12 MeV the  $A_y(\theta)$  near 125° is very sensitive to the magnitude of the  $^3P$  interaction. This is exhibited in Fig. 2 (top half) where calculations are shown for three cases in which each  $^3P$  interaction was turned off separately. The relative insensitivity of  $A_y(\theta)$  to the magnitude of the  $^1P$  and D interactions is shown in the bottom half of Fig. 2. The discrepancy between the full PEST calculation and the data in the angular region near 125°

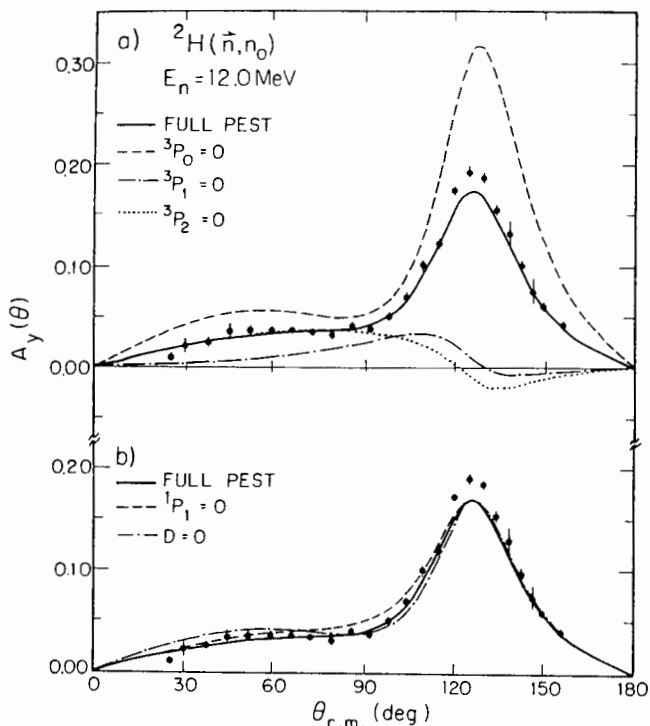


Fig. 2 Measured analyzing power (dots) for n-d scattering at 12 MeV. The solid curves are a calculation based on the Paris NN potential.

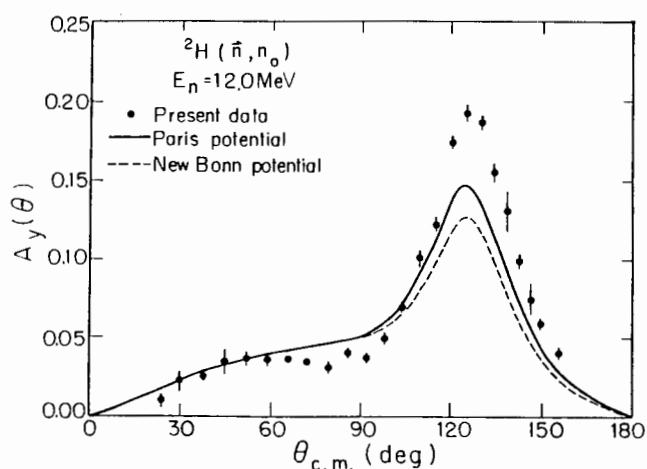


Fig. 3 Measured analyzing power (dots) for n-d scattering at 12 MeV. The solid and dashed curves are rigorous calculations using the Bonn and Paris NN interactions, respectively.

indicates that either the  $^3P$  interaction of the Paris NN potential must be modified or perhaps there is evidence for 3NF effects, effects which are not explicitly included in the Paris potential.

In addition to testing the semi-phenomenological Paris potential, the n-d scattering data is clearly important in the on-going development of the Bonn field-theoretical model. We have been collaborating with the theoretical group at Bochum which has developed a method<sup>2</sup> of performing rigorous calculations from the

potentials directly, thereby avoiding the need for constructing separable potentials. Their 12 MeV calculations<sup>2</sup> using the Paris and Bonn potentials are compared to  $A_y(\theta)$  data from TUNL in Fig. 3. Considering the complexity of the Bochum calculation, the prediction is encouraging. Here again, we see that the Bonn potential leads to an inferior description of the data. Recalling the sensitivities shown in Fig. 2, we conclude that the  $^3P$  NN interaction of the Bonn potential probably needs to be investigated carefully.

#### Nucleon Scattering from $^{28}\text{Si}$

One of our major goals involves the derivation of macroscopic potentials to simultaneously describe neutron and proton scattering from identical nuclei. Following the direction introduced by A.M. Lane, this is possible if one properly describes the isospin interaction and all of the Coulomb effects. Intimately tied to this problem is the magnitude of the charge-symmetry breaking interaction. A serious problem that arises in fitting neutron and proton data simultaneously is the ambiguities between the asymmetry terms and the so-called Coulomb correction terms,  $\Delta V_c$  and  $\Delta W_c$ , which are introduced to convert a neutron-nucleus potential into a proton-nucleus potential. Determination of the Coulomb effects is simplified in the case of  $T=0$  targets, for then the asymmetry term, which is proportional to  $(N-Z)/A$ , is zero. The example to be shown here involves such a nucleus,  $^{28}\text{Si}$ . We have obtained  $\sigma(\theta)$  and  $A_y(\theta)$  data for  $n + ^{28}\text{Si}$  in the energy range from 8 to 17 MeV and have combined these data with published  $\sigma(\theta)$  data from 20 to 40 MeV and total cross section  $\sigma_T$  data from 1 to 50 MeV.

The analysis proceeded stepwise. First, a coupled-channels (CC) analysis for  $n + ^{28}\text{Si}$  was conducted for the ground ( $0^+$ ), first excited ( $2^+$ ) and second excited ( $4^+$ ) states of  $^{28}\text{Si}$ . Initially, single-energy searches were conducted to obtain geometry parameters and the spin-orbit potential. These quantities were then averaged. Next, we conducted single-energy searches for the strengths of the real central and surface imaginary potentials,  $V_R$  and  $W_D$ , respectively. The strength of the volume imaginary potential  $W_V$  was held to a linear energy dependence that was deduced in a preliminary analysis<sup>8</sup>. A comparison between the calculations and the data is shown in Figs. 4 and 5. The results for the potentials (Set A) are shown as points in Fig. 6. To allow for systematic investigations, a set of potential strengths (Set B) was obtained by fitting a linear curve to the discrete values of Set A. (See Fig. 6.) The Set B predictions are shown by the dashed curves in Figs. 4 and 5. It is clear from Fig. 4 that additional high accuracy data in the 26 to 40 MeV region would help establish if the bump in  $W_D$  observed in the discrete, single-energy searches is real.

Available  $p + ^{28}\text{Si}$  data for  $E_p$  from

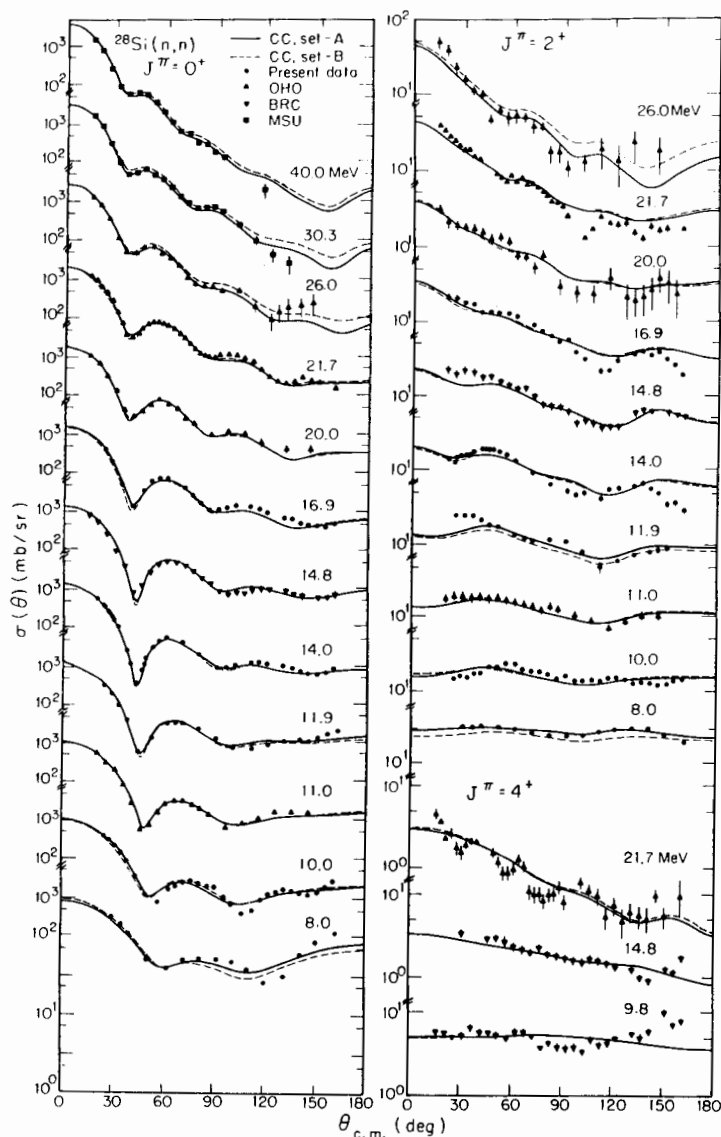


Fig. 4 The  $\sigma(\theta)$  for elastic and inelastic scattering of neutrons from  $^{28}\text{Si}$ . The curves are CC calculations which model  $^{28}\text{Si}$  as a symmetric rotor. The data at 30 and 40 MeV are from ref. 10, at 9.8, 11, 20, 22 and 26 MeV from Ohio University, at 14.8 MeV from Bruyères-le-Châtel and at 8, 10, 12, 14 and 17 MeV from TUNL.

15 to 40 MeV were fit next using the same geometry and spin-orbit parameters as derived in the neutron case. Reasonable agreement with the data was obtained for two different approaches for determining the Coulomb correction term  $\Delta V_c$ . In the first case, the data were searched upon with no pre-determined constraint on  $\Delta V_c$ . The results for  $V_R$  for the single-energy searches are shown in Fig. 7. Least-square fits to the data indicate similar linear energy dependences, with a value of  $\Delta V_c = 0.33$  MeV, corresponding to the difference in the intercepts for the neutron and proton curves. A small Coulomb correction  $\Delta W_c$  was obtained for the imaginary potential. Our value for  $\Delta V_c$  is much less than the typical value of 1.8 MeV expected from Coulomb barrier considerations according to the method of Perey<sup>9</sup> ( $\Delta V_c = 0.4 Z/A^{1/3}$ ) and the value of 1.65 MeV from a study by Winfield et al.<sup>10</sup> who matched up the structure in the diffraction pattern for neutrons from  $^{28}\text{Si}$  with that for protons at nearby energies. In the second case, the real potential strengths were computed by shifting the linear function of Set B, which was deduced by fitting the neutron data, down in energy by an amount  $\Delta E_c$  to correct for the

slowing down of the incident proton due to the Coulomb repulsion of the nucleus. The value of  $\Delta E_c$  used in this analysis was 5.7 MeV and was derived by Winfield et al.<sup>10</sup> using the method mentioned above. The fits to the proton data were optimized at each energy by searching on  $W_D$  and  $W_V$ . The resulting volume integrals per nucleon  $J_W/A$  (volume plus surface) for the imaginary potentials are denoted as Set E and are shown in Fig. 8. Here the proton values have been graphed for a beam energy reduced by  $\Delta E_c = 5.7$  MeV. Comparison with the values from parameter Set A of the neutron analysis (see Fig. 8) led to the unexpected result that the  $J_W/A$  were nearly identical for both projectiles after shifting the proton values down in energy by the 5.7 MeV. This finding suggests that a potential for proton scattering from  $^{28}\text{Si}$  can be derived by shifting the functions which represent the energy dependencies of the real and imaginary parts of the corresponding neutron-scattering potential down in energy by an amount  $\Delta E_c$  obtained by "lining up" the diffraction patterns for neutrons and protons<sup>10</sup>.

In conclusion, neutron and proton measurements for scattering from  $^{28}\text{Si}$

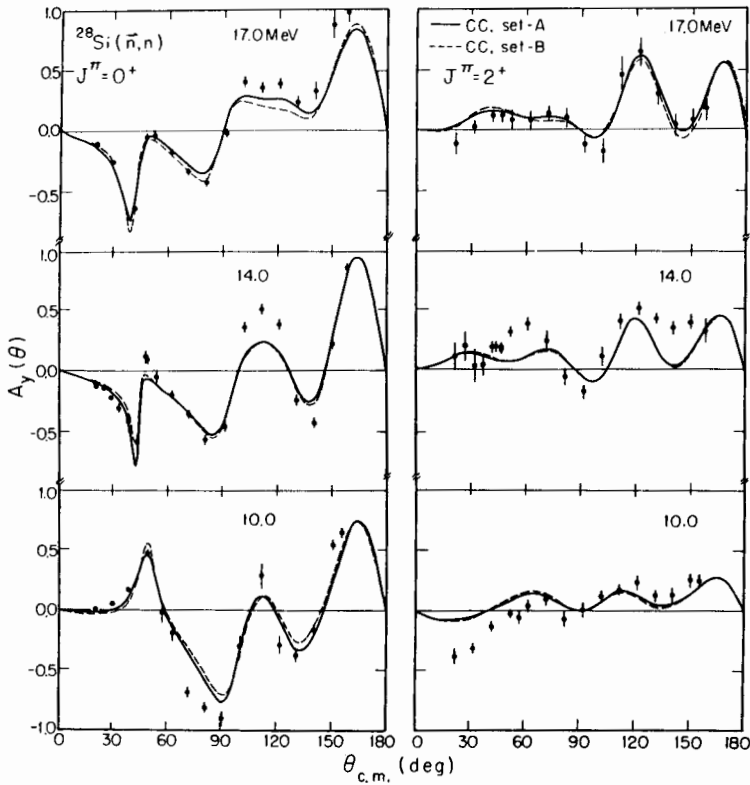


Fig. 5 The  $A_y(\theta)$  data obtained at TUNL for elastic and inelastic scattering of neutrons from  $^{28}\text{Si}$ .

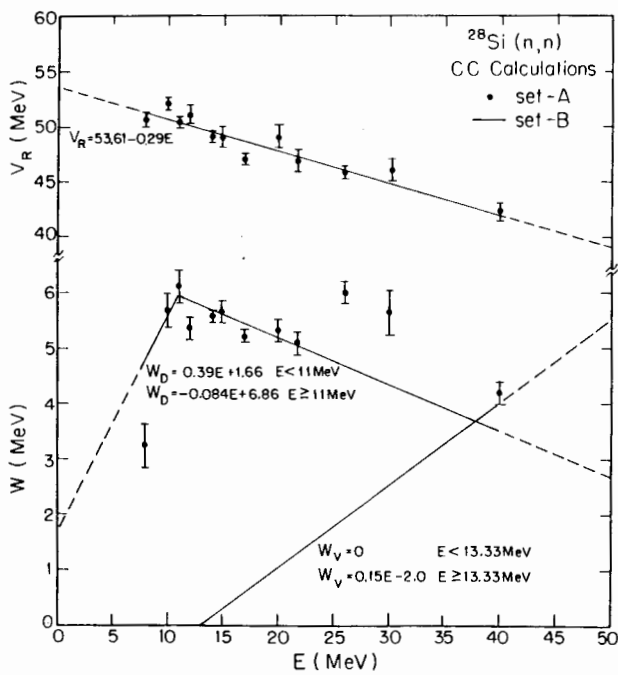


Fig. 6 Potential strengths of the real and imaginary wells. The points are the results of single-energy searches on  $V_R$  and  $W_D$ . Parameter set B is a linear least-square fit to the points. The dashed extensions are extrapolations based on fitting neutron total cross sections.

Fig. 8 Comparison of volume integrals per nucleon for imaginary potentials for neutron and proton scattering. The proton points have been shifted by  $\Delta E_c = 5.7$  MeV to account for the energy loss due to Coulomb repulsion.

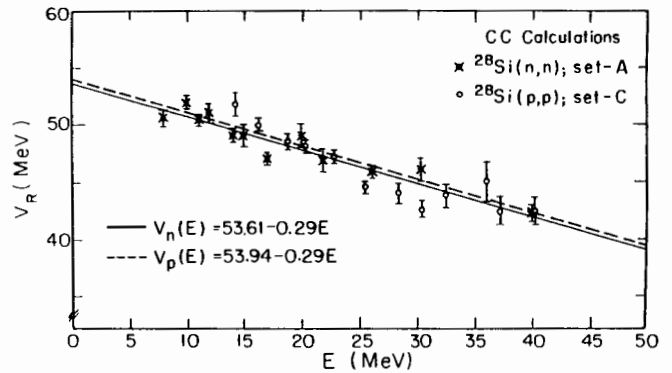
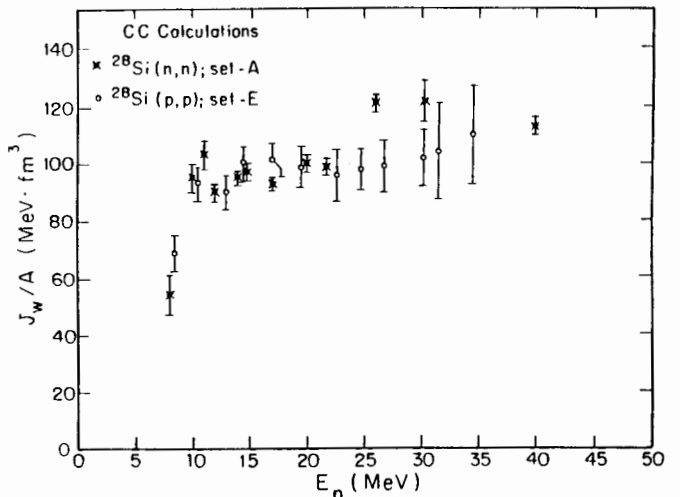


Fig. 7 Potential strengths of the real well versus incident projectile energy. The solid and dashed lines are least-square fits to the neutron and proton potential points, respectively.



scattering data can be described with the same potential. However, there are two equally satisfactory ways of introducing the Coulomb effects. The proton potential can be derived by adding a term  $\Delta V_C = 0.33$  MeV and a small term  $\Delta W_C$  to the respective neutron potentials, or it can be derived by using values for the real and imaginary potential strengths of the neutron potential at an energy reduced by  $\Delta E_C = 5.7$  MeV, which amounts to a  $\Delta V_C = 1.65$  MeV for the real potential. This ambiguity in trading off the effects of the Coulomb interaction between the real and imaginary potentials causes at least a 1.3 MeV uncertainty in determining  $\Delta V_C$ . Such a large uncertainty means that one should reconsider the magnitude of the charge-symmetry-breaking term deduced from the  $\Delta V_C$  determination reported earlier<sup>10</sup>. Here also we note that the strength of the combined n and p analysis would be enhanced if  $A_y(\theta)$  and better  $\sigma(\theta)$  data were available for n + <sup>28</sup>Si between 25 and 40 MeV.

We have made similar studies for many nuclei ranging from <sup>6</sup>Li to <sup>120</sup>Sn, but for most cases the only neutron data for energies above 26 MeV is  $\sigma_T$  data. For more convincing analyses in these cases also, it would be useful to have some higher energy  $\sigma(\theta)$  and  $A_y(\theta)$  neutron data.

#### Neutron Scattering from <sup>208</sup>Pb and <sup>209</sup>Pb

Several aspects of the nuclear potential for the interaction of neutrons with <sup>208</sup>Pb are being reinvestigated with the addition of detailed and high accuracy  $A_y(\theta)$  measurements recently obtained at TUNL. One aspect deals with the report of Annand et al.<sup>11</sup> who found the need to introduce an energy-dependent radius for the real potential when they attempted to describe primarily  $\sigma(\theta)$  data from 4 to 26 MeV with a spherical optical model (SOM). Their characterization of the radius produced a volume integral  $J_V$  which increased abnormally as  $E_n$  decreased. Shortly thereafter this feature was claimed to give evidence for a surface contribution to the real central potential, a contribution expected from the dispersion relation between the surface imaginary potential and the real potential. Several interesting and detailed articles<sup>12</sup> have followed this seminal report.

In order to test these claims and also to confine the potential descriptions more tightly, we have made high-accuracy measurements of  $A_y(\theta)$  in the critical energy range from 6 to 10 MeV. We have combined these data with  $\sigma(\theta)$  data and attempted a spherical optical model (SOM) analysis<sup>13</sup> to find a solution which describes in detail all the systematics of the  $\sigma(\theta)$  and  $A_y(\theta)$  data. No satisfactory SOM solution based on conventional Woods-Saxon (WS) form factors could be found, even allowing for a surface term for the real potential.

Presently we are concentrating on the 8-MeV data and trying other form factors. We use the Fourier-Bessel (FB) expansion method to relax the constraint of having a

WS form factor for each term of the potential. The main observation is that the real central potential must be modified. In fact, when the shapes of all but the real central potential  $V(r)$  are held to WS or derivative WS form factors, the data can be explained quite well. The results for  $\sigma(\theta)$  and  $A_y(\theta)$  are shown in Fig. 9. (In the FB computer code the Mott-Schwinger electromagnetic interaction, which causes a large  $A_y(\theta)$  at far forward angles, is not included. To account for this limitation, it is necessary to adjust the data a slight bit using corrections estimated with an SOM code which calculates  $A_y(\theta)$  either with or without this interaction. For all the <sup>208</sup>Pb data shown, the data include this adjustment.) The  $V(r)$  resulting from the FB expansion is shown in Fig. 10 in comparison to the underlying WS-shaped potential that gives the best fit when only WS form factors are used. Unfortunately, this FB solution is not unique; the obtained shape depends upon the number of terms used in the FB expansion. We are now studying the form factors of  $V(r)$  at other energies with the aim of establishing a definite systematic pattern for  $V(r)$  as a function of energy. It seems that in the single-energy searches adding an FB contribution to the surface imaginary term is not advantageous, but when the 6- to 10-MeV data are searched upon simultaneously, such a term helps to reduce the total chi-squared.

We had hoped to make a definitive statement about the spin-orbit potential for n + <sup>208</sup>Pb in this paper. To do so would be premature. However, the current situation is as follows: i) Adding FB terms to the conventional derivative WS form factor for the spin-orbit potential does not give a significant improvement to the data. ii) Single-energy SOM searches from 6 to 10 MeV using pure WS forms for all potentials give the following range of values:  $5.7 < V_{SO} < 7.1$  (MeV),  $0.96 < r_{SO} < 1.25$  (fm) and  $0.32 < a_{SO} < 0.61$  (fm). iii) A combined search on the 6- to 10-MeV data gives an energy independent potential having  $V_{SO} = 6.39$  MeV,  $r_{SO} = 1.206$  fm and  $a_{SO} = 0.530$  fm.

In 1981 we reported<sup>14</sup> our first  $A_y(\theta)$  data for elastic scattering from Fe and Cu and in 1983 from <sup>208</sup>Pb<sup>15</sup>. In order to describe the data with an optical model calculation, it was necessary to introduce an imaginary spin-orbit term  $W_{SO}$  having a strength of about +1 MeV at  $E_n = 10$  MeV. This need has surfaced in other cases that we have studied, and it seems to be there in both the SOM and coupled-channels (CC) approach. With the new, more accurate and more complete <sup>208</sup>Pb data we have found that the need for this term in an SOM description (and in a preliminary CC description) persists when conventional WS form factors are employed. Our conclusions about  $W_{SO}$  when FB adjustments are made to the form factors are not definite yet. To show the sensitivity to this term, the results (solid curve) of an FB search at 8 MeV when a  $W_{SO}$  of +0.8 MeV was used are compared in Fig. 11 to calculations (dashed curve) with the same

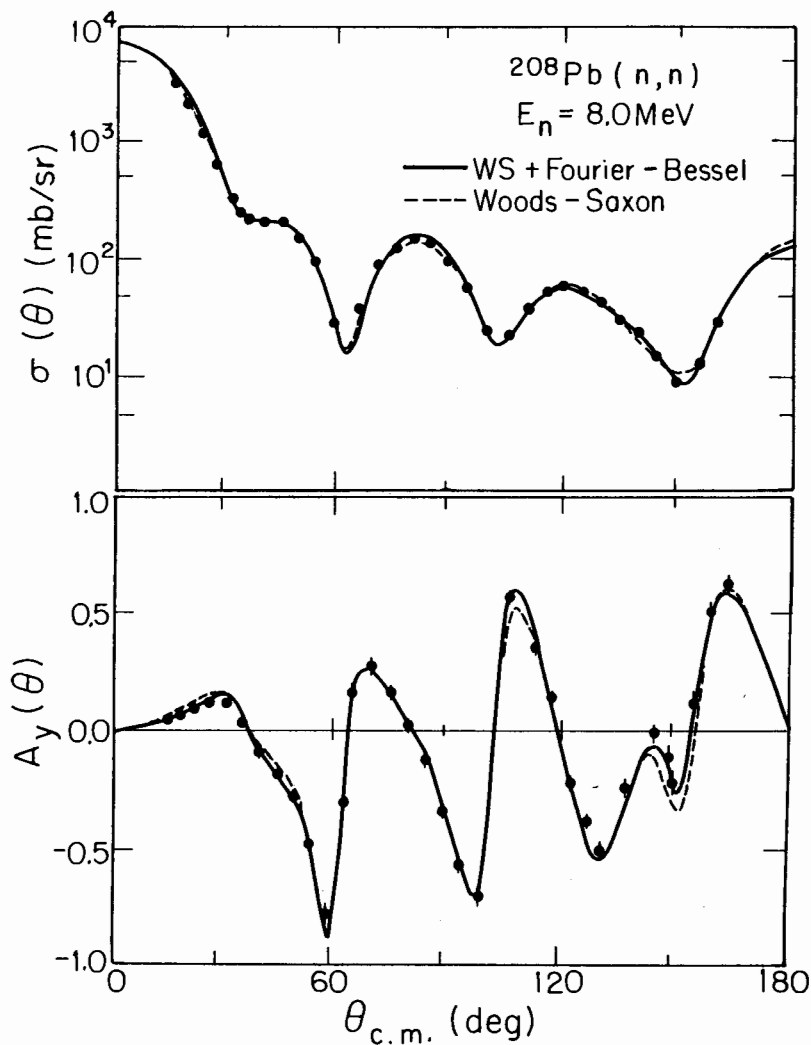


Fig. 9 Measurements of  $\sigma(\theta)$  and  $A_y(\theta)$  for  $^{208}\text{Pb}(n,n)$  scattering. The curves are SOM calculations performed with a Fourier-Bessel-series contribution added to the Woods-Saxon real potential term  $V(r)$ .

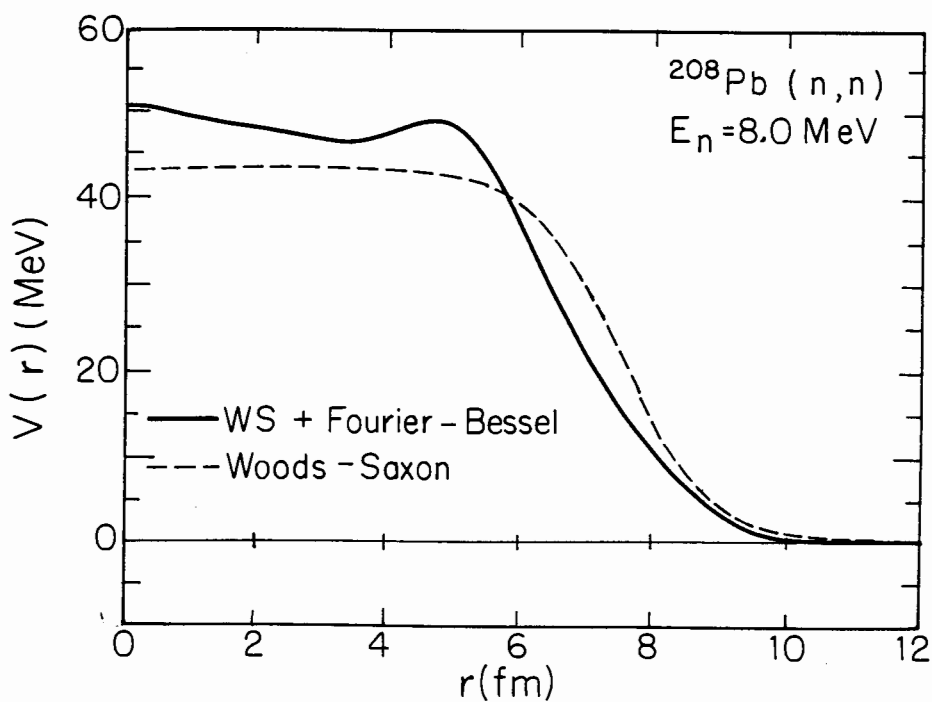


Fig. 10 The form factor of  $V(r)$  derived in the Fourier-Bessel analysis (solid curve) of the 8 MeV data for  $^{208}\text{Pb}(n,n)$ . The dashed curve is the Woods-Saxon form factor derived in a conventional SOM analysis of the same data.

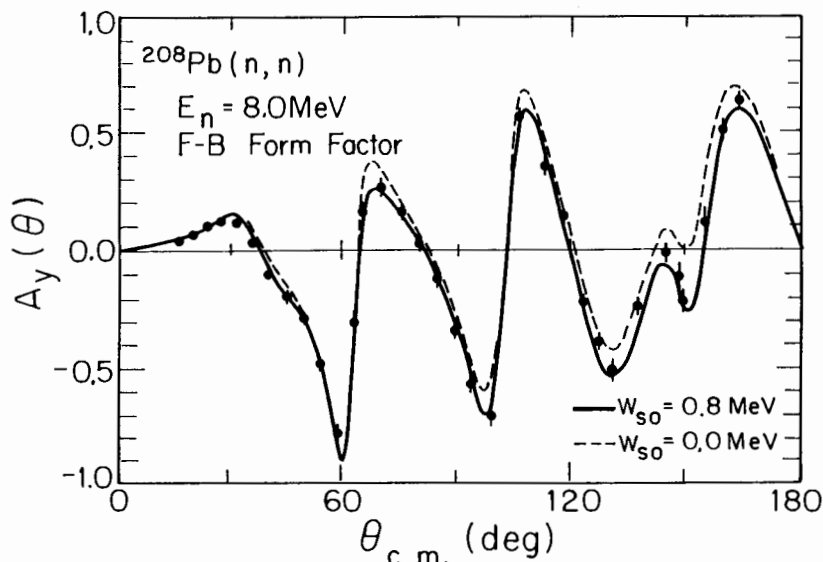


Fig. 11 Sensitivity of SOM with and without including the imaginary spin-orbit interaction. (See text.)

potentials when  $W_{so}$  is set to zero. At this stage though it is too early to conclude whether an acceptable set of FB form factors can be formed that will give an equally good fit with  $W_{so} = 0$ . Although the introduction of the dispersion relation<sup>16,17</sup> may have eliminated the need for  $W_{so}$  for  $n$ -<sup>40</sup>Ca, so far we have not found this approach to be sufficient in the case for <sup>208</sup>Pb.

Implicit in our <sup>208</sup>Pb analysis is the assumption that the compound elastic scattering can be calculated with adequate accuracy. Since the  $A_y(\theta)$  is zero for the compound nucleus (CN) contribution (when averaged over many resonances), the effect of the CN yield is to dilute the structure in the  $A_y(\theta)$  distribution produced by the shape elastic contribution. The CN contribution is small above 8 MeV for <sup>208</sup>Pb but is very significant at 6 MeV. In order to increase the level of confidence in our ability to make accurate CN predictions, we have performed  $A_y(\theta)$  measurements for <sup>209</sup>Bi as well. These were done at 9 MeV, an energy where the CN contribution is negligible, and at 6 MeV where there is some CN contribution, but where the CN cross section is much less than that for <sup>208</sup>Pb. At 9 MeV the measured  $A_y(\theta)$  for <sup>208</sup>Pb and <sup>209</sup>Bi are essentially identical; the small differences probably can be attributed to the small change associated with the conventional radial dependence  $R = r_0 A^{1/3}$ . Large differences were observed between the <sup>208</sup>Pb and the <sup>209</sup>Bi data at 6 MeV. Unfortunately, although the CN contribution is less for <sup>209</sup>Bi because of the higher level density, the minima in the shape-elastic differential cross section at 6 MeV also turned out to be lower for <sup>209</sup>Bi than for <sup>208</sup>Pb. This feature must be due to differences in the energy dependence in the SOM parameters for these two nuclei; an accurate description of the <sup>209</sup>Bi data should shed more light on the CN calculations for both nuclei and on the dispersion relation terms and the energy dependencies of  $J_V$  and the potential radii for <sup>208</sup>Pb.

We gratefully acknowledge the support of our students and collaborators who have participated in the measurements and conducted analyses and theoretical calculations. This work is supported by the U.S. Department of Energy, Office of High Energy and Nuclear Physics, under Contract No. DE-AC05-76ER01067.

#### REFERENCES

1. C.R. Gould et al.: Phys. Rev. Lett. **57**, 2371(1986)
2. H. Witala, W. Glöckle and T. Cornelius: Suppl. to Few-Body Systems **2**, 555(1987)
3. R. Machleidt, K. Holinde and Ch. Elster: Phys. Report **149**, 1(1987)
4. R.A. Arndt: private communication
5. M. Lacombe et al.: Phys. Rev. **C21**, 861(1980)
6. W. Tornow et al.: Phys. Rev. C (in press)
7. C.R. Howell et al.: Few-Body Systems **2**, 19(1987)
8. C.R. Howell: Proc. of the Conf. on Neutron-Nucleus Collisions - A Probe of Nuclear Structure, Burr Oak State Park, Ohio, 1984, AIP Conf. Proc. No. 124
9. F.G. Perey: Phys. Rev. **131**, 745(1963)
10. J.S. Winfield et al.: Phys. Rev. **C33**, 1(1986)
11. J.R.M. Annand, R.W. Finlay and F.S. Dietrich: Nucl. Phys. **A443**, 249(1985)
12. C.H. Johnson, D.J. Horen and C. Mahaux: Phys. Rev. **C36**, 2252(1987) and refs. therein
13. M.L. Roberts et al.: Bull. Am. Phys. Soc. **33**, 1061(1988)
14. C.E. Floyd et al.: Phys. Rev. **C47**, 1042(1981)
15. J.P. Delaroche et al.: Phys. Rev. **C28**, 1410(1983)
16. J.P. Delaroche and W. Tornow: Phys. Lett. **B203**, 4(1988)
17. C.H. Johnson and C. Mahaux: (submitted to Phys. Rev. C)